Pathologic characterization of white striping myopathy in broiler chickens

Francesco Prisco,[*] Davide De Biase,[*] Giuseppe Piegari,[*] Ilaria d'Aquino,[*] Adriano Lama,[†] Federica Comella,[†] Raffaelina Mercogliano,[‡] Ludovico Dipineto,[§] Serenella Papparella,[*] and Orlando Paciello[*,1]

[*]*Department of Veterinary Medicine and Animal Production, Unit of Pathology, University of Naples Federico II, Via F. Delpino 1, 80137 Napoli, Italia;* [†]*Department of Pharmacy, School of Medicine, University of Naples Federico II, Via Domenico Montesano 49, 80131, Napoli, Italia;* [‡]*Department of Veterinary Medicine and Animal Production, Unit of Food Inspection, University of Naples Federico II, Via F. Delpino 1, 80137 Napoli, Italia; and* [§]*Department of Veterinary Medicine and Animal Production, Unit of Avian Diseases, University of Naples Federico II, Via F. Delpino 1, 80137 Napoli, Italia*

ABSTRACT White striping (**WS**) is an emerging myopathy of broiler chickens characterized by white striation of muscle. Despite the recent advances, the pathomechanism underlying the WS remains elusive.

The aim of this study was to characterize morphological and molecular features of WS in broiler chickens. 50 pectoralis muscles were collected from 55 days old ROSS 308 broiler chickens with a mean weight of 3.5 kg. Samples were snap frozen and analyzed by histopathology, immunohistochemistry, and immunofluorescence. Real-time-PCR was used to evaluate the expression of different cytokines.

Histological lesions were observed in all examined animals, both with and without macroscopic evidence of WS. WS muscles showed endomysial and perivascular inflammatory infiltrates of macrophages and cluster of differentiation (**CD**)8-positive T lymphocytes with severe myofiber atrophy, necrosis, fibrosis and replacement by adipose tissue. There was diffuse sarcoplasmic and sarcolemmal overexpression of the major histocompatibility complex class I (**MHC I**). The severity of the histologic lesions was positively correlated with the macroscopic degree of white striations. IL-6, IL-17 and lipopolysaccharide-induced TNF-α factor (**LITAF**) were overexpressed in severe lesions of WS. The presence of the CD8/MHC I complexes, together with the higher expression of IL-6, IL-17 and LITAF in severe degree of WS, suggest that the immune response may be involved in the progression of this myopathy and can be consistent with a hypoxia-induced inflammatory myopathy. These results help to understand the pathomechanism of WS contributing to the reduction of economic losses and improving poultry welfare.

Key words: immune-mediated disease, musculoskeletal, myositis, poultry, autoimmunity

2021 Poultry Science 100:101150
https://doi.org/10.1016/j.psj.2021.101150

INTRODUCTION

The increase in demand for chicken meat has been accompanied by intense genetic selection for growth rate, but on the other hand it is accompanied by a variety of challenges, one of which is the white striping myopathy (**WS**) (Kuttappan et al., 2016; Boerboom et al., 2018). WS is an emerging disease in broiler chickens, macroscopically characterized by white striations of the pectoralis and thighs muscles parallel to the muscle fibers (Kuttappan et al., 2017). WS is considered an esthetic and technological defect that devalues broiler breast filets (Zanetti et al., 2018). Many studies reported that the incidence of WS in broiler chickens increased dramatically from an average of 5% in 2012 (Huang and Ahn, 2018) to over than 90% in the last years (Kuttappan et al., 2017; Malila et al., 2018), with considerable economic losses for the poultry industry (Zanetti et al., 2018).

There is little information available regarding the histological lesions associated with WS myopathy. The few studies have focused on abnormalities that can influence the chemical and textural properties of the meat, such as fibrosis and replacement with adipose tissue, and these studies only occasionally report microscopic changes such as necrosis and infiltration of lymphocytes and macrophages (Kuttappan et al., 2013; Salles et al., 2019; Praud et al., 2020).

Received January 13, 2021.
Accepted March 10, 2021.

[1]Corresponding author: paciello@unina.it

To date, the pathomechanisms underlying WS are unclear. Recent studies suggested that hypoxia plays a major rule in WS pathogenesis (Boerboom et al., 2018; Malila et al., 2019); however, oxidative stress, fiber-type switching, and nutritional deficiencies may also contribute (Boerboom et al., 2018). There is little information about the characteristics of the inflammatory response in WS (Zambonelli et al., 2016). Increasing evidence indicates that inflammatory responses including macrophages and T helper 17 ($\mathbf{T_H17}$) cell responses play a pivotal role in modulating the neovascularization, repair and remodeling after muscle ischemia (Hata et al., 2011; Chen et al., 2018). For this reason, in addition to the morphological characterization of the inflammatory infiltrate, in the present study we explored the T helper 1 ($\mathbf{T_H1}$)/T_H17 polarization of the inflammatory response.

Moreover, different ischemic injuries, such as myocardial infarctions (Liao and Cheng, 2006), stroke and traumatic brain injury (Javidi and Magnus, 2019), have been recently associated with immune-mediated disorders. In an ischemia-induced inflammatory microenvironment, self-reactive lymphocytes and autoantibodies could be generated and may participate in inflammation and in the progression of tissue injury (Liao and Cheng, 2006; Javidi and Magnus, 2019). Based on these observations, we hypothesized that an immune-mediated component may be part of the pathogenesis of WS. For this reason, in the present study, we evaluated the presence of the CD8/MHC I complexes, as hallmarks of immune-mediated muscle diseases, and assessed the expression of cytokines related to immune-mediated diseases (Pagano et al., 2019; Prisco et al., 2020).

The aims of this study were to 1) characterize the histologic and histoenzymatic features of WS, 2) characterize the inflammatory infiltrate, 3) evaluate the expression of CD8/MHC I complexes, and 4) assess cytokine expression in order to understand the pathomechanisms underlying this myopathy.

MATERIALS AND METHODS

Samples

The study included pectoralis muscles from 50 commercial broiler chickens (ROSS 308) randomly selected from five batches raised at a facility of a local poultry meat producer. Broilers were slaughtered with 55 d of age and with a mean weight of 3.5 Kg at a CE authorized slaughterhouse. The study did not require consent or ethical approval according to European Directive 2010/63/EU. The animals were slaughtered in strict accordance with European slaughter regulations (CE n° 1099/2009 of 24 September 2009) for the protection of animals at the time of killing (Ref. Official Journal of the European Union L 303/1). Permission to obtain the samples was granted from the owner of the abattoir and from the veterinary inspector responsible for sanitary surveillance.

The gross severity of WS was graded in chicken pectoralis muscles following an established method (Malila et al., 2018):

- Grade 0 (non-WS): no white striation on the meat surface;
- Grade 1 (mild-WS): 1 to 40 white lines with a thickness of < 1 mm;
- Grade 2 (moderate-WS): more than 40 white lines with a thickness of < 1 mm, or 1 to 5 white lines with a thickness of 1 to 2 mm;
- Grade 3 (severe-WS): more than 5 white lines with a thickness of 1 to 2 mm, or at least one line with a thickness ≥ 2 mm.

The WS severity of the breast muscles was graded by 2 independent pathologists (F.P. and O.P.). Discordant results were reviewed to reach consensus.

For this study we avoided samples with wooden breast, "spaghetti meat", and deep pectoral (green muscle disease) myopathies (Bailey et al., 2015). Within 20 min postmortem, two samples were collected from the cranial region on the ventral surface of each breast muscle, one of which was placed in RNAlater. All samples were immediately transported under refrigeration (2−4°C) to the Comparative Neuromuscular Laboratory of the Department of Veterinary Medicine of the University of Naples within 1 to 2 hours after sampling. Samples of $1 \times 1 \times 1$ cm were snap-frozen in isopentane precooled in liquid nitrogen for histology and the aliquots transported in RNAlater were frozen at −80°C for molecular examination.

Histopathology and Immunohistochemistry

Frozen transverse sections (8-μm thick) were stained according to our routinely performed laboratory stains (Paciello and Papparella, 2009) including: 1) hematoxylin and eosin (**HE**) and 2) Engel trichrome (**ET**) for a basic morphologic evaluation and mitochondria distribution; 3) reduced nicotinamide adenine dinucleotide-tetrazolium reductase (**NADH-TR**) to observe intermyofibrillar pattern and secondary distribution of mitochondria; and iv) succinate dehydrogenase (**SDH**) and v) cytochrome oxidase (**COX**) to evaluate activity and distribution of mitochondria (Paciello and Papparella, 2009).

A scoring system was designed to assess the degree of fiber atrophy as follows based on assessment of at least 10 fields at 200X magnification (9.503 mm^2; 20× objective and a 10× ocular with a field number of 22 mm) (Meuten et al., 2016): normal (score 0), no atrophic fibers; mild (score 1), <10% atrophic fibers; moderate (score 2), 10% to 50% atrophic fibers; and severe (score 3), >50% of atrophic fibers. (Pagano et al., 2015, 2019; Costagliola et al., 2016) Fibers were considered atrophic if the diameter was lower than 36 μm which is the minimum reported value for the cranial portion of the pectoral muscle of broiler chicken at slaughter-age (Smith and Fletcher, 1988; Dubowitz et al., 2013).

The number of inflammatory cells were scored by light microscopy as: no infiltration (score 0); mild infiltration (score 1), on average 5 to 25 inflammatory cells per high-power field (**HPF**; 0.237 mm^2; 40× objective and a 10×

ocular with a field number of 22 mm) (Meuten et al., 2016); moderate infiltration (score 2), on average 26 to 50 inflammatory cells per HPF; and severe infiltration (score 3), on average more than 50 inflammatory cells per HPF. The average number was evaluated in at least 10 HPF for each sample (Pagano et al., 2019).

The degree of fiber necrosis was scored as follows based on assessment of at least 10 fields at 200× magnification: normal (score 0), no necrotic fibers; mild (score 1), <10% necrotic fibers; moderate (score 2), 10% to 50% necrotic fibers; and severe (score 3), >50% of necrotic fibers (Pagano et al., 2015; Costagliola et al., 2016). For the evaluation of fiber necrosis, both the fibers with loss of the normal sarcoplasm structure and the necrotic fibers invaded by macrophages (sarcoclastosis) were counted (Dubowitz et al., 2013; Pagano et al., 2019).

Fibrous and adipose tissue replacement were separately scored as follows using a system based on the assessment of 10 field at 200× magnification: normal (score 0) no fibrous/adipose tissue replacement; mild (score 1), <10% of the skeletal muscle is replaced by fibrous/adipose tissue; moderate (score 2), 10% to 20% is replaced; and severe (score 3), >20% is replaced.

The alterations of intermyofibrillar pattern and alterations in mitochondrial activity and distribution has been studied with histoenzymatic stains to mark the following oxidative enzyme activities: reduced nicotinamide adenine dinucleotide-tetrazolium reductase, and COX (Dubowitz et al., 2013; Pagano et al., 2019). A scoring system was designed to assess the degree of alteration of intermyofibrillar pattern and alteration in mitochondrial activity and distribution. This score was based on the percentage of fibers showing abnormalities with the NADH-TR, SDH, and COX stains, such as coarse intermyofibrillar pattern, "moth-eaten" fibers, target fibers, targetoid fibers, core fibers, pre-ragged blue fibers, whorled fibers etc. The score was assessed on at least 10 fields at 200× magnification: normal (score 0), no evident alteration; mild (score 1), <10% of fibers showed morphological alterations; moderate (score 2), 10% to 20% of fibers showed morphological alterations; and severe (score 3), >20% of fibers showed morphological alterations.(Pagano et al., 2015; Costagliola et al., 2016; Zaghini et al., 2020)

Sections were evaluated by 2 independent pathologists (F.P. and O.P.) under an optical microscope (Nikon E600; Nikon, Tokyo, Japan). Discordant results were reviewed with a multiheaded microscope to reach consensus.

For immunohistochemistry (**IHC**), frozen sections (8-μm thick) were processed with the MACH1 Universal HPR Polymer Detection Kit (Biocare Medical LLC, Concord, CA) as previously described (Pagano et al., 2019). The primary antibodies used are summarized in Table 1. A quantitative assessment of immunohistochemical stained sections was performed on 5 randomly selected cases for each grade of severity of the gross lesions. For each case, ten 20× fields were randomly photographed under an optical microscope (Leica DM6000B by Leica, Wetzlar, Germany) associated with a digital camera (Leica DFC450C digital camera by Leica). Each photo was elaborated with Fiji (ImageJ, National Institutes of Health): a color deconvolution filter (H DAB) was applicated to each photo to permit discrimination of browns and blues; the obtained 8-bit browns level was binarized using a threshold manually adjusted (between 0−100 and 0−120), as needed, for each image sets to accurately reflect chromogen distribution in the regions of interest; and the positive area was measured (Johnson and Walker, 2015; Law et al., 2017; Cimmino et al., 2019). The mean positive area of the 10 analyzed field was calculated for each case and expressed in percentage of the area of an entire field (% units). Furthermore, the areas of the marked inflammatory cells were added to obtain, for each case, a total inflammatory cell area. The mean positive areas of the 5 selected cases were calculated for each group of macroscopic severity.

Table 1. Anti-chicken monoclonal antibodies used as primary antibodies for immunohistochemistry and immunofluorescence.[1]

Recognized chicken molecule	Target	Clone	Dilution
Bu-1	B lymphocytes	AV20	1:400
CD3	T lymphocytes	CT−3	1:100
CD4	T helper lymphocytes	CT−4	1:100
CD8α	T cytotoxic lymphocytes	CT−8	1:500
TCR$\gamma\delta$	$\gamma\delta$-T lymphocytes	TCR-1	1:200
Monocyte/ Macrophage-antigen	Monocyte/Macrophage	KUL01	1:500
MHC I	Major histocompatibility complex class I	F21−2	1:500
MHC II	Major histocompatibility complex class II	2G11	1:500

[1]All primary antibodies were mouse monoclonal antibody from SouthernBiotech, Birmingham, AL, USA.

Immunofluorescence

To determine if muscle fibers infiltrated by CD8+ lymphocytes expressed Major histocompatibility complex class I (**MHC I**; CD8/MHC I complexes), immunofluorescence was carried out as follows. Cryosections were dried at room temperature for 1 hour, preincubated with normal mouse serum diluted 1:10, and overlaid overnight in a humid chamber at 4°C with primary antibody for MHC Class I (F21−2, mouse monoclonal antibody, dilution 1:500; SouthernBiotech). A TRITC fluorochrome-labeled rabbit anti-mouse secondary antibody was applied (1:300; Jackson Laboratories, Bar Harbor, ME, USA) on sections for 1 h at room temperature. Slides were rinsed with PBS and a second primary antibody directed against CD8 (CT−8, mouse monoclonal antibody, dilution 1:400; SouthernBiotech) was applied overnight at 4°C. A FITC fluorochrome-labeled rabbit anti-mouse secondary antibody was applied (1:300; Jackson Laboratories) on sections for 2 h at room temperature. Slides were rinsed with PBS and mounted with a solution of 1-part glycerol/1-part PBS. For scanning and photography was used a fluorescence

microscope (Leica DM6000B by Leica, Wetzlar, Germany) associated with a digital camera (Leica DFC450C digital camera by Leica). To exclude autofluorescence, serial sections of muscle were incubated with PBS omitting the primary antibody. Frozen sections of normal chicken cecal tonsils were used as positive controls for anti-MHC I and anti-CD8 antibodies.

RNA Extraction and Real-Time Semiquantitative PCR

To explore the T_H1/T_H17 inflammatory response and to evaluate the expression of cytokines related to immune-mediated diseases, total RNA derived from 5 pectoralis muscles randomly selected for each severity grade was extracted using TRIzol Reagent (Bio-Rad Laboratories) using a specific RNA extraction kit (NucleoSpin®, MACHEREY-NAGEL GmbH & Co, Düren, Germany), according to the manufacturer's instructions. cDNA was synthesized using High-Capacity cDNA Reverse Transcription Kit (Applied Biosystems) from 6 μg total RNA. The applied PCR settings were previously described (Lama et al., 2019). The gene primers were: IFNG (for IFN-γ), **LITAF** (for lipopolysaccharides-induced TNF-alpha factor), IL6 (for IL-6), IL12A (for IL-12A), IL17 (for IL-17) (Qiagen, Hilden, Germany) in a final volume of 25 μL. All mRNAs were normalized to GAPDH as housekeeping gene, and data were analyzed according to the $2^{-\Delta\Delta C}{}_T$ method (De Biase et al., 2020).

Statistical Analysis

Statistical analysis was performed using Prism 8 (Version 8.2.1) with a level of significance of 0.05. The D'Agostino-Pearson test was used to assess normality of data. The differences among means of each histologic semiquantitative score were evaluated using Kruskal−Wallis test and a post-hoc multiple comparison using Dunn's test (Meyerholz et al., 2019). The differences among means of immunohistochemical quantitative assessments and Real-time PCR quantitative assessments were evaluated using one-way analysis of variance (ANOVA) and a post-hoc multiple comparison using the Holm-Sidak's multiple comparisons test (Aickin and Gensler, 1996).

The following correlations were evaluated using the Spearman's rank correlation coefficient: 1) the macroscopic grade of the WS vs histologic semiquantitative scores and the immunohistochemical quantitative assessments; 2) among the various histologic semiquantitative scores; 3) between histologic semiquantitative scores vs. immunohistochemical quantitative assessments. The size of correlation coefficient has been interpreted as "low" for correlation coefficients lower than 0.5; "moderate" for correlation coefficients between 0.5 and 0.7; and "high" for correlation coefficients higher than 0.7 (Mukaka, 2012).

RESULTS

Gross Examination

White striations were present in 45 of 50 (90%) samples, with characteristic white striations parallel to the muscle fibers and more severe lesions in the cranio-lateral parts of the pectoralis muscles where the muscles were thicker (Figure 1A). The other 5 of 50 pectoralis muscle samples were macroscopically normal (grade 0).

Grade 1 (mild) lesions were present in 20 of 0 (40%) pectoralis muscles, with few and thin (< 1 mm) white striations usually exclusively present in the cranio-lateral parts of the pectoralis muscles. Grade 2 (moderate) lesions were present in 16 of 50 (32%) of the pectoralis muscles, with numerous white striations some of which were 1 to 2 mm, and usually more evident in the cranial two-thirds of the pectoralis muscles. Grade 3 (severe) lesions were present in 9 of 50 (18%) of the pectoralis muscles, several white striations, some thicker than 2 mm, usually evident in the whole pectoralis muscle

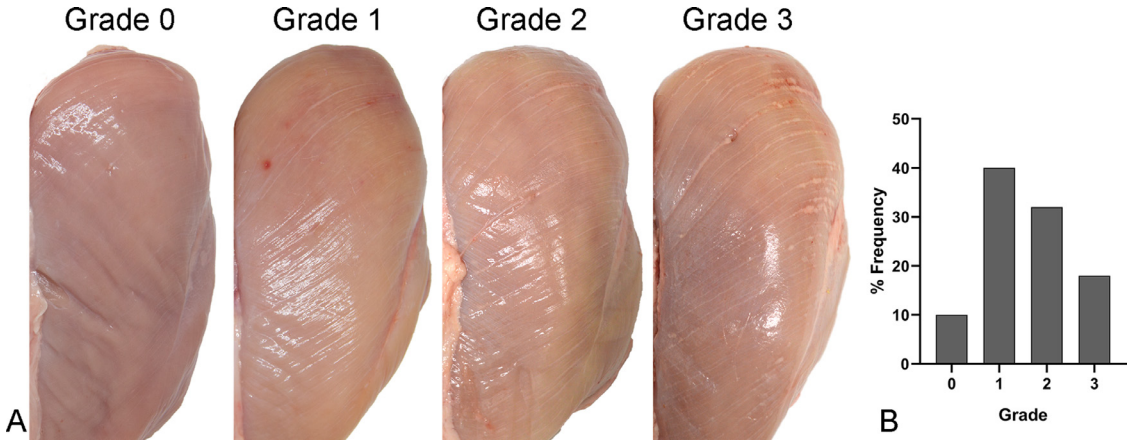

Figure 1. Gross findings. (A) White striping myopathy (WS), left pectoralis major muscle, chicken. Scoring scale used for evaluation of histopathologic changes. Muscles classified as grade 0 (normal, case 3) not show any distinct white lines. Muscles classified as grade 1 (mild, case 7) exhibit white lines, less than 1 mm thick, parallel to the muscle fibers. Muscles classified as grade 2 (moderate, case 35) exhibit white lines from 1 to 2 mm thick, parallel to the muscle fibers. Muscles classified as score 3 (severe, case 44) exhibit easily evident white lines, more than 2 mm thick, parallel to the muscle fibers and associated with hemorrhages on the muscle surface. (B) Gross lesion scores for WS in pectoralis muscles from 50 broiler chickens. Only 10% of the muscles were morphologically normal and the most frequent lesions score was grade 1.

and often associated with hemorrhages. Distribution data are summarized in Figure 1B.

Histology and Immunohistochemistry

Atrophy, inflammation, necrosis, fibrosis and adipose tissue replacement were prominent findings in all cases. Other associated myopathic features were centralization of nuclei, fiber splitting, and endomysial and perimysial edema.

There was increased variability of muscle fiber diameter with numerous muscle fibers reduced in size (atrophy), mainly round, rarely with angular profiles, scattered or distributed in small groups. The atrophy was scored as mild in 8 of 50 (16%) cases, moderate in 26 of 50 (52%) cases, and severe in 16 of 50 (32%) cases (Figure 2A).

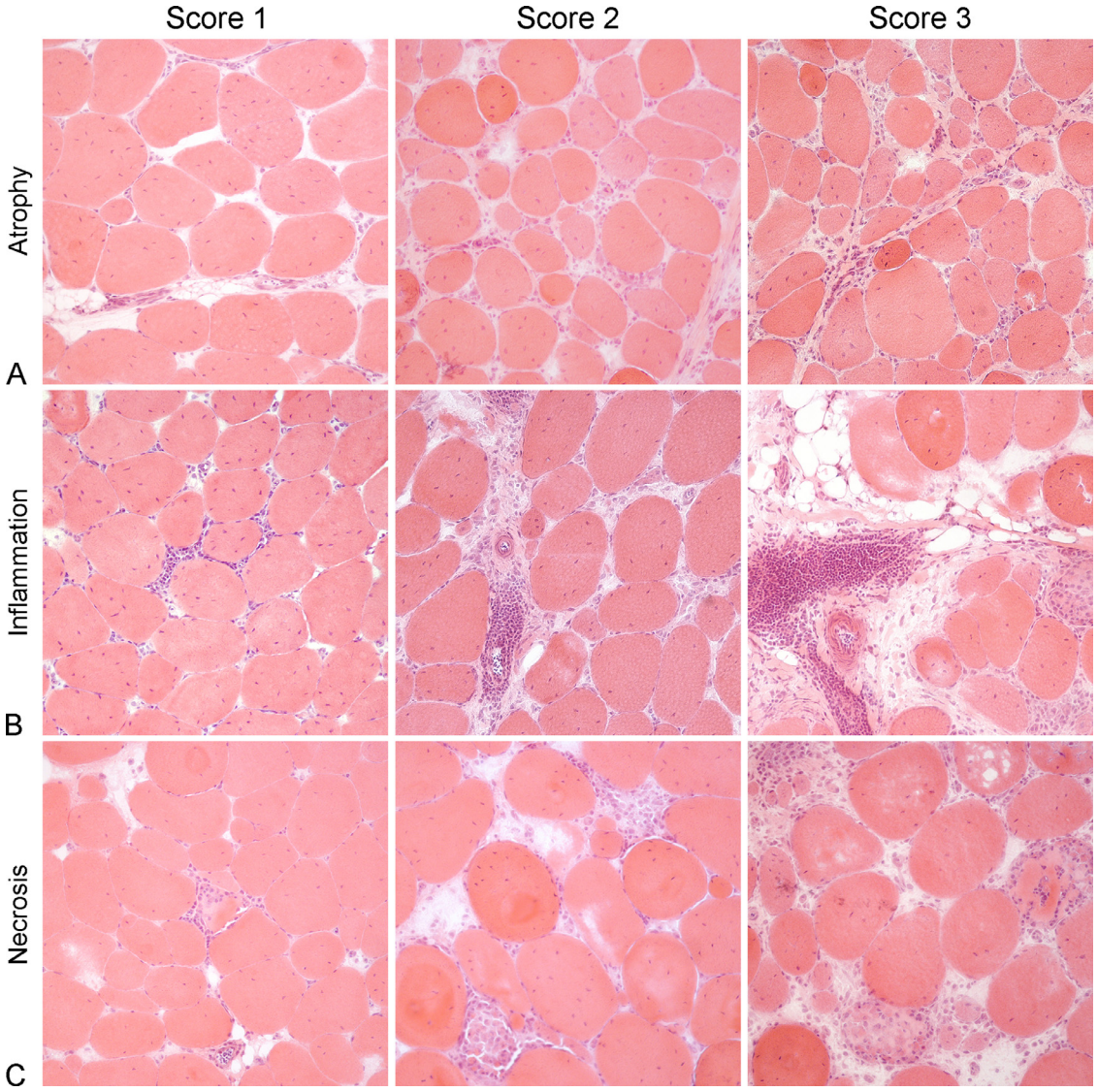

Figure 2. Histologic findings. (A) Atrophy, white striping myopathy (WS), skeletal muscle, chicken. Muscle fiber diameters are variable with numerous fibers reduced in size (atrophy). Atrophic fibers are mainly round or rarely had angular profiles. Hematoxylin and eosin (HE). Atrophy Score 1: Case 5, Mild atrophy (<10% atrophic fibers), centralization of muscle fibers nuclei, endomysial edema and scattered inflammatory cells. Atrophy Score 2: Case 16, Moderate atrophy (10%−50% atrophic fibers), centralization of muscle fibers nuclei, endomysial fibrosis and infiltrating inflammatory cells. Atrophy Score 3: Case 35, Severe atrophy (>50% of atrophic fibers), centralization of muscle fibers nuclei and severe inflammatory cells infiltration in the endomysium. (B) Inflammation, WS, skeletal muscle, chicken. Infiltrates of lymphocytes and macrophages expand the endomysium and surround and infiltrate among muscle fibers. HE. Inflammation Score 1: Case 2, Mild inflammation (5−25 inflammatory cells per HPF), centralization of muscle fibers nuclei and endomysial edema. Inflammation Score 2: Case 31, Moderate inflammation (26−50 inflammatory cells per HPF), centralization of muscle fibers nuclei, scattered atrophic fibers and perimysial fibrosis. Inflammation Score 3: Case 42, Severe inflammation (>50 inflammatory cells per HPF), centralization of muscle fibers nuclei, perimysial fibrosis and replacement with adipose tissue. Inset: the inflammatory infiltrate is composed by lymphocytes and macrophages. (C) Myofiber necrosis, WS, skeletal muscle, chicken. Necrotic fibers are present, and are invaded by inflammatory cells, mainly macrophages. HE. Necrosis Score 1: Case 9, Mild myofiber necrosis (<10% necrotic fibers) with sarcoclastosis, centralization of muscle fibers nuclei, scattered atrophic fibers and scattered inflammatory cells in the endomysium. Necrosis Score 2: Case 24, Moderate myofiber necrosis (10%−50% necrotic fibers) with sarcoclastosis, centralization of muscle fibers nuclei, scattered atrophic fibers and scattered inflammatory cells in the endomysium. Necrosis Score 3: Case 40, Severe myofiber necrosis (>50% of necrotic fibers) with sarcoclastosis, centralization of muscle fibers nuclei, scattered atrophic fibers and endomysial edema.

All examined cases showed endomysial and perivascular infiltration of macrophages, lymphocytes, and plasma cells. Endomysium was multifocally expanded by numerous macrophages, which often invaded necrotic muscle fibers (sarcoclastosis), associated with fewer lymphocytes and plasma cells, and often surrounding intact myofibers. Rarely, morphologically normal muscle fibers were infiltrated by one or few lymphocytes. Furthermore, numerous blood vessels were surrounded by lymphocytes and plasma cells, often organized in follicular structures, with fewer macrophages. Sometimes, inflammatory cells infiltrated and disrupted the vessel walls. Lymphoplasmacytic and histiocytic inflammation was scored as mild in 14 of 50 (28%) cases, moderate in 15 of 50 (30%) cases, and severe in 21 of 50 (42%) cases (Figure 2B).

Often, frequent scattered muscle fibers were necrotic and invaded by numerous macrophages (sarcoclastosis). The number of necrotic fibers was scored as mild in 14 of 50 (28%) cases, moderate in 22 of 50 (44%) cases and severe in 14 of 50 (28%) cases (Figure 2C).

Fibrous and adipose tissue replacement of the skeletal muscle was also prominent. Fibrous replacement was absent in 3 of 50 (6%) cases, mild in 17 of 50 (34%) cases, moderate in 16 of 50 (32%) cases, and severe in 14 of 50 (28%) cases (Figure 3A). Adipose tissue replacement was absent in 3 of 50 (6%) cases, mild in 9 of 50 (18%) cases, moderate in 21 of 50 (42%) cases, and severe in 17 of 50 (34%) cases (Figure 3B).

Abnormalities of the intermyofibrillar pattern and mitochondrial activity and distribution were present in 49 of 50 cases, including coarse intermyofibrillar pattern and mitochondrial abnormalities such as "moth eaten" fibers, target fibers, targetoid fibers, core fibers, preragged blue fibers, and whorled fibers. Abnormalities of intermyofibrillar pattern and activity and distribution of mitochondria were scored as absent in 1 case (2%), mild in 15 of 50 (30%) cases, moderate in 25 of 50 (50%) cases and severe in 9 of 50 (19%) cases (Figure 3C).

The atrophy score was higher in muscle with grade 3 WS compared with grade 0 ($P< 0.05$). Inflammation score was higher in muscle with grade 3 WS compared with grade 0 ($P < 0.05$) and grade 1 ($P< 0.05$). Necrosis score was higher in muscle with grade 3 WS compared with grade 0 ($P< 0.01$), grade 1 ($P< 0.05$), and grade 2 ($P< 0.05$). Fibrosis score was higher in grade 3 WS compared with grade 0 ($P< 0.01$) and grade 1 ($P< 0.01$). Fibrosis score was higher also in grade 2 WS compared with grade 0 ($P < 0.05$). Adipose tissue replacement score was lower in grade 0 WS compared with grade 3 ($P< 0.001$), grade 2 ($P< 0.01$) and grade 1 ($P< 0.05$). Mitochondrial alteration score was higher in muscle with grade 3 WS compared with grade 1 WS ($P < 0.05$) and grade 0 WS ($P< 0.01$). The differences between mean scores are summarized in Figure 4.

The grade of gross severity of the WS was moderately positively correlated with fibrosis score ($r_s = 0.621$; $P< 0.001$), adipose tissue replacement score ($r_s = 0.530$; $P< 0.001$) and mitochondrial alteration score ($r_s = 0.515$; $P < 0.001$) and was lowly positively correlated with atrophy score ($r_s = 0.325$; $P< 0.05$), inflammation score ($r_s = 0.411$; $P< 0.01$) and necrosis score ($r_s = 0.480$; $P< 0.001$). Atrophy score was highly positively correlated with inflammation ($r_s = 0.757$; $P< 0.001$) and necrosis ($r_s = 0.757$; $P< 0.001$) scores, was moderately positively correlated with fibrosis score ($r_s = 0.545$; $P< 0.001$) and mitochondrial alteration score ($r_s = 0.603$; $P< 0.001$) and lowly positively correlated with adipose tissue replacement ($r_s = 0.434$; $P< 0.01$) score. Inflammation score was also highly positively correlated with necrosis score ($r_s = 0.814$; $P< 0.001$), moderately positively correlated with fibrosis score ($r_s = 0.579$; $P< 0.001$), and mitochondrial alteration score ($r_s = 0.663$; $P< 0.001$) and lowly positively correlated with adipose tissue replacement score ($r_s = 0.470$; $P= 0.001$). Necrosis score was moderately positively correlated with fibrosis score ($r_s = 0.639$; $P< 0.001$), adipose tissue replacement score ($r_s = 0.568$; $P= 0.001$) and mitochondrial alteration score ($r_s = 0.654$; $P< 0.001$). Fibrosis score was moderately positively correlated with mitochondrial alteration score ($r_s = 0.585$; $P< 0.001$) and lowly positively correlated with adipose tissue replacement score ($r_s = 0.436$; $P= 0.01$). Adipose tissue replacement score was also lowly positively correlated with mitochondrial alteration score ($r_s = 0.479$; $P < 0.001$).

The inflammatory infiltrate expanding the endomysium and invading the necrotic muscle fibers was mainly composed of macrophages with fewer CD8+ lymphocytes and scattered or small groups of CD4+ lymphocytes, Bu1+ B cells and TCR$\gamma\delta$+ lymphocytes. Otherwise, the inflammatory infiltrate surrounding the blood vessels was mainly composed of CD3+ T lymphocytes, predominantly CD8+ with less CD4+, associated with fewer Bu1+ B cells, TCR$\gamma\delta$+ lymphocytes and macrophages (Figure 5A).

The quantitative assessment of immunolabeled sections (Figure 5B) showed that the overall inflammatory population was mainly composed of macrophages and CD8+ lymphocytes. Furthermore, the distribution of the inflammatory infiltrate by each grade (Figure 5C) showed that for all markers the mean immunolabeling increased from grade 0 to grade 2 and decreased from grade 2 to grade 3. The exception was that immunolabeling of macrophages continuously increased from grade 0 to grade 3.

TCR$\gamma\delta$ immunolabeling was higher in grade 3 WS compared with grade 0 ($P< 0.05$) and was higher in grade 2 compared with grade 0 ($P< 0.01$) and grade 1 ($P< 0.05$). MAC immunolabeling was higher in grade 3 compared with grade 0 ($P< 0.001$) and grade 1 ($P< 0.0001$) and was higher in grade 2 compared with grade 0 ($P<0.01$).

The macroscopic grade of the WS was highly positively correlated with MAC positivity ($r_s = 0.845$; $P< 0.001$) and with total inflammatory cells ($r_s = 0.717$; $P= 0.001$). Furthermore, macroscopic grade was moderately positively correlated with CD4 positivity ($r_s = 0.605$; $P<$

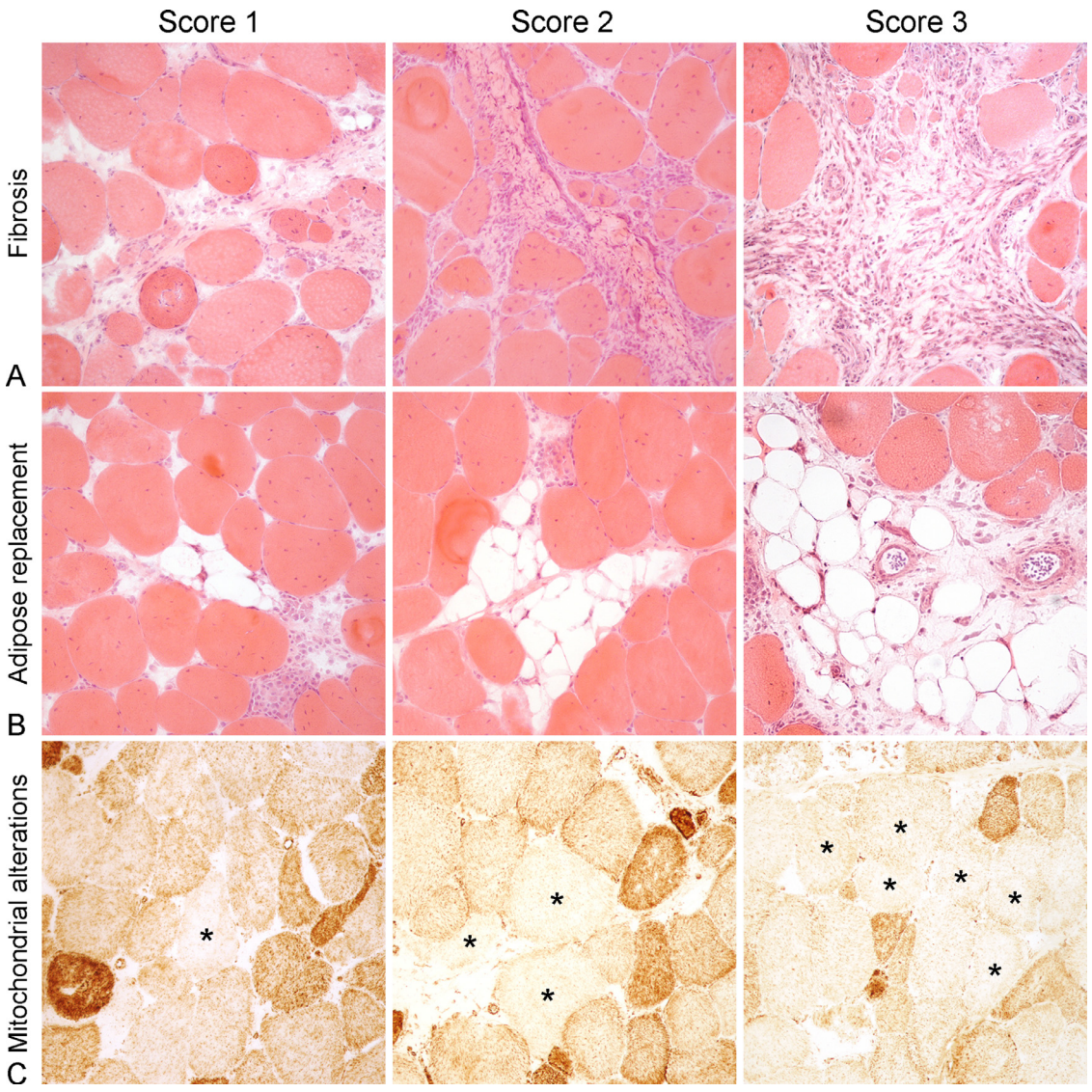

Figure 3. Histologic findings. (A) Fibrosis, White striping myopathy, skeletal muscle, chicken. The endomysium is expanded by fibrous tissue. HE. Fibrosis Score 1: Case 23, Mild fibrosis (<10% of the skeletal muscle replaced), centralization of muscle fibers nuclei, scattered atrophic fibers and endomysial edema. Fibrosis Score 2: Case 19, Moderate fibrosis (10%−20% of the skeletal muscle replaced), centralization of muscle fibers nuclei, small groups of atrophic fibers and infiltration of inflammatory cells. Fibrosis Score 3: Case 43, Severe fibrosis (>20% of the skeletal muscle replaced), centralization of muscle fibers nuclei, scattered atrophic fibers and severe infiltration of inflammatory cells. (B) Adipose tissue replacement, WS, skeletal muscle, chicken. The endomysium and perimysium are expanded by adipose tissue. HE. Adipose tissue replacement Score 1: Case 9, Mild replacement with adipose tissue (<10% of the skeletal muscle replaced), centralization of muscle fibers nuclei, necrosis with sarcoclastosis of a single muscle fiber and focal infiltration of inflammatory cells. Adipose tissue replacement Score 2: Case 20, Moderate replacement with adipose tissue (10%−20% of the skeletal muscle replaced), centralization of muscle fibers nuclei, necrosis with sarcoclastosis of a single muscle fiber and scattered inflammatory cells infiltrating the endomysium. Adipose tissue replacement Score 3: Case 26, Severe replacement with adipose tissue (>20% of the skeletal muscle replaced), centralization of muscle fibers nuclei and scattered inflammatory cells infiltrating the perimysium. (C) Mitochondrial alterations, WS, skeletal muscle, chicken. Diffusely pale fibers (asterisks) show the absence of COX activity. Cytochrome oxidase stain. Mitochondrial alterations Score 1: Case 10, Mild reduction in staining for cytochrome oxidase (<10% of fibers). Mitochondrial alterations Score 2: Case 40, Moderate reduction in staining for cytochrome oxidase (10% to 20% of fibers). Mitochondrial alterations Score 3: Case 47, Severe reduction in staining for cytochrome oxidase (>20% of fibers).

0.01), Bu-1 positivity ($r_s = 0.523$; $P < 0.05$) and TCR$\gamma\delta$ positivity ($r_s = 0.690$; $P = 0.001$).

Sarcolemmal and sarcoplasmic immunopositivity for MHC I was constantly observed in at least 90% of muscle fibers in all cases, both in fields with and without an evident inflammatory infiltrate. Sarcolemmal and sarcoplasmic immunopositivity for MHC II were never observed (Figure 6A).

Immunofluorescence

To explore the possible overexpression of MHC I on the sarcolemma of the non-necrotic muscle fibers infiltrated by CD8-positive lymphocytes, immunofluorescence was performed. In all cases, the intact myofibers infiltrated by CD8-positive lymphocytes showed an intense sarcolemmal and diffuse sarcoplasmic

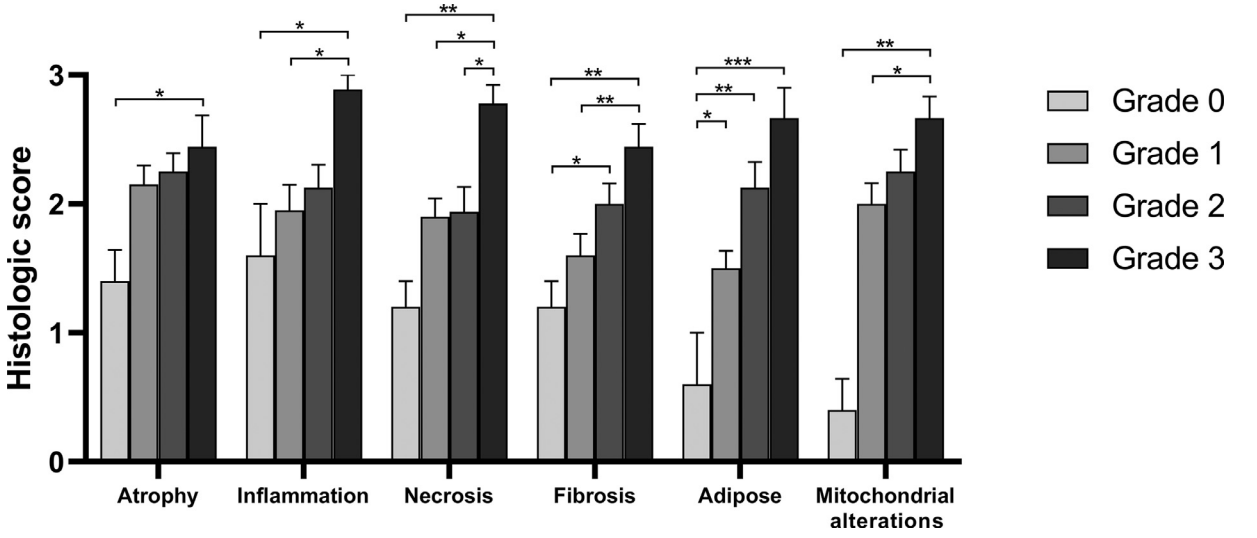

Figure 4. Relationships between histological lesion scores and macroscopic severity grade in muscles samples from 50 broiler chickens. Scores were determined for the histologic lesions shown and compared among samples with different macroscopic severity grades (grades 0-3, shown by different colored bars). The histological lesions were progressively more severe according to the macroscopic severity grade of the white striping. Bars indicate means ± SEM. The means were compared using the Kruskal−Wallis test and post-hoc Dunn's multiple comparison. Asterisks denote statistically differences between macroscopic lesions grades ($^{*}P < 0.05$, $^{**}P < 0.01$, $^{***}P < 0.001$).

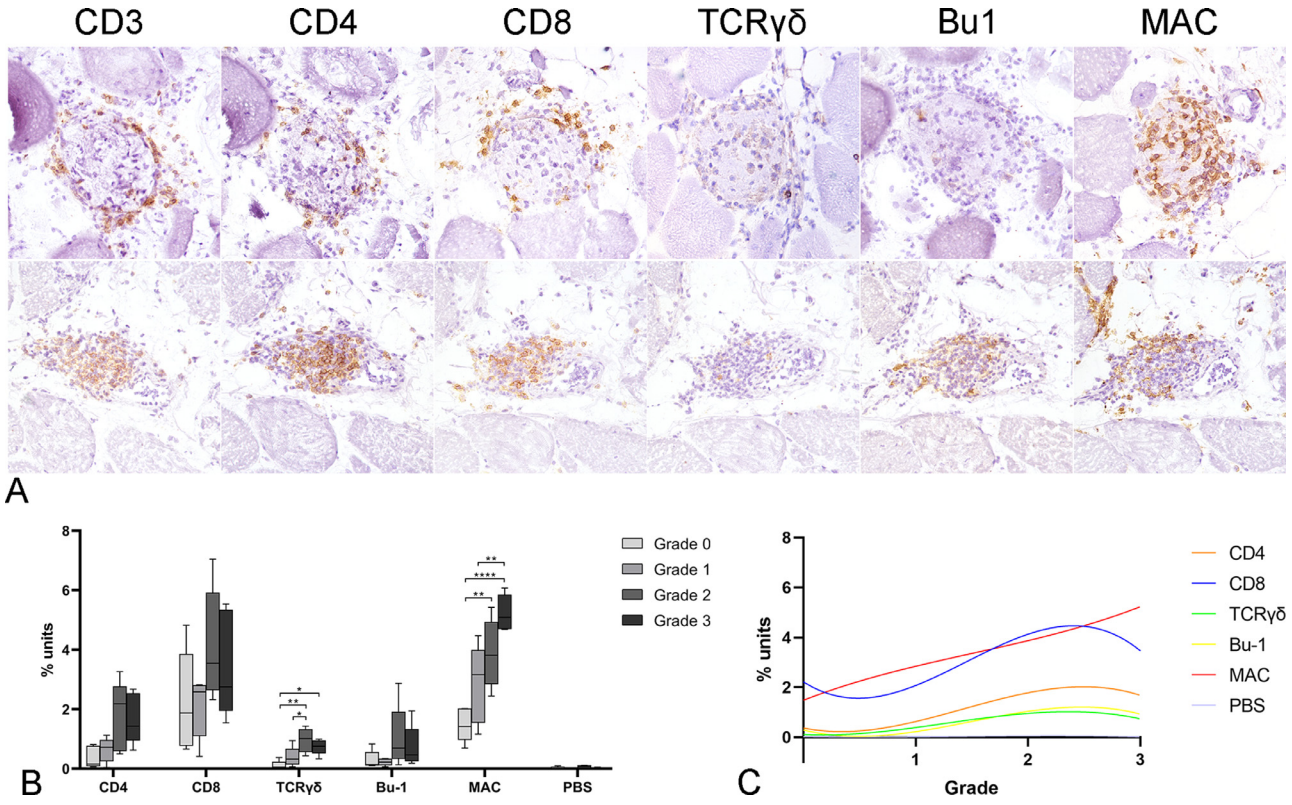

Figure 5. Immunohistochemical findings. (A) White striping myopathy, skeletal muscle, chicken. Detection of CD3, CD4, CD8, TCR$\gamma\delta$, Bu1 and MAC on serial cryosection. The endomysial inflammatory infiltrate is mainly composed of macrophages with fewer CD8+ lymphocytes. There are scattered CD4+ lymphocytes, Bu1+ B cells, and TCR$\gamma\delta$+ lymphocytes (top row; Case 26). The perivascular inflammatory infiltrate is mainly composed of CD3+ lymphocytes, with both CD8+ and CD4+ cells. There are a moderate number of Bu1+ B cells and macrophages and few TCR$\gamma\delta$+ lymphocytes (bottom row; Case 6). (B) Quantitative assessment of immunolabeling. The inflammatory cell population was mainly composed of macrophages and CD8+ lymphocytes. Immunolabeling for most markers increased from macroscopic lesion grade 0 to grade 2 and decreased from grade 2 to grade 3. The exception was Immunolabeling for macrophages (MAC), which continually increased from grade 0 to grade 3. Five cases from each macroscopic lesion grade were tested (20 cases in total). Means were compared with one-way ANOVA and post-hoc Holm-Sidak's multiple comparison. Asterisks denote statistically differences between grades ($^{*}P < 0.05$, $^{**}P < 0.01$, $^{***}P < 0.001$, $^{****}P < 0.0001$). (C) Immunohistochemical data trends according to macroscopic grade. Nonlinear regression. MAC positivity had the best positive correlation with macroscopic grade (r_s=0.845; $P < 0.001$; Spearman's rank correlation coefficient).

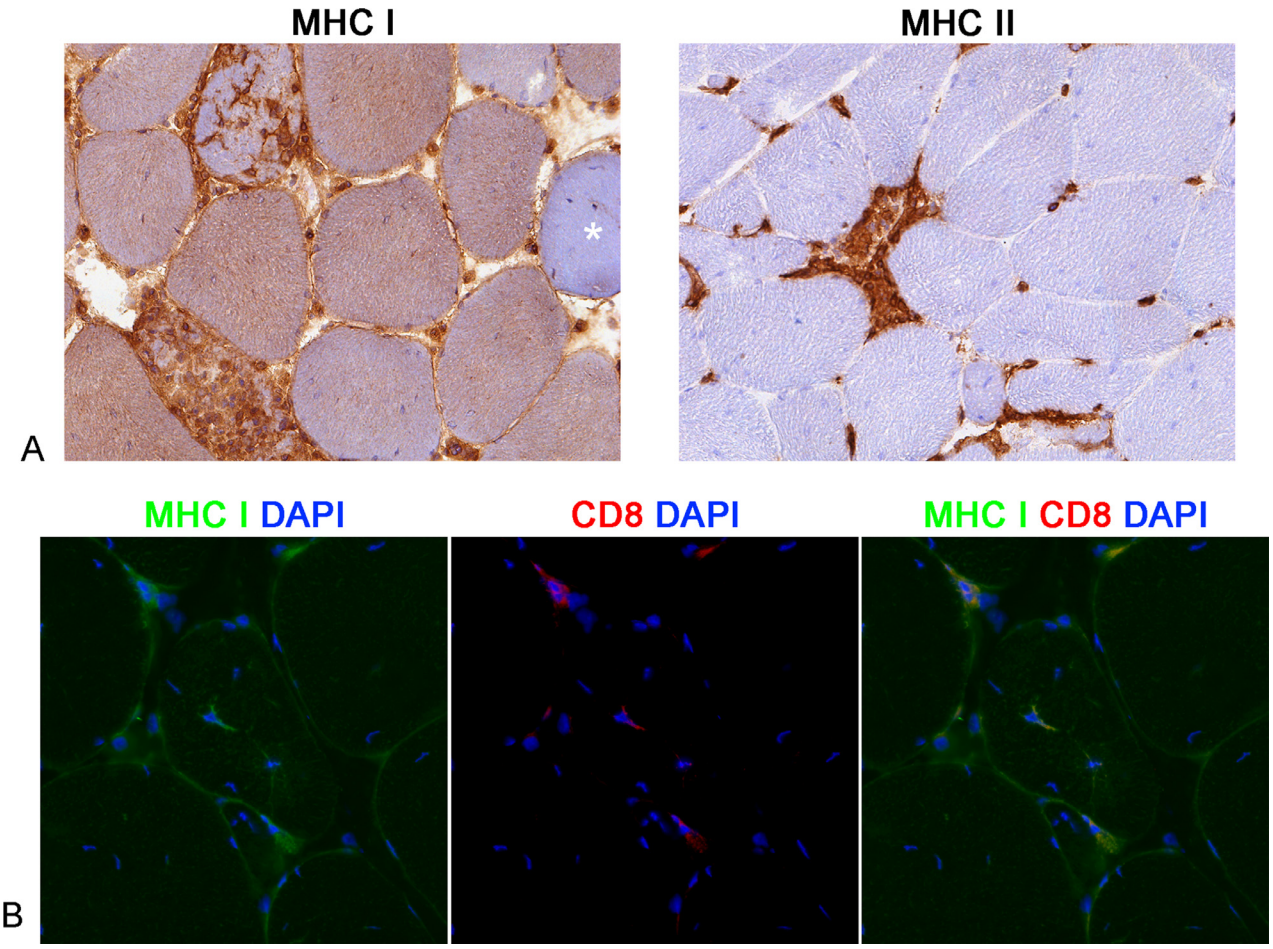

Figure 6. MHC I and MHC II expression. (A) White striping myopathy, skeletal muscle, chicken. Immunohistochemistry. Almost all muscle fibers diffusely overexpress MHC I both on the sarcolemma and in the sarcoplasm. Negative muscle fibers are rare (asterisk; Case 9). The infiltrating inflammatory cells and the endothelial cells of the endomysial capillaries are MHC II-positive but no muscle fibers are positive (Case 9). (B) White striping myopathy, skeletal muscle, chicken. Immunofluorescence detection labeling of CD8 (green, FITC), MHC I (red, TRIC), and their colocalization (merge, orange color). Muscle fibers exhibit diffuse sarcolemmal and cytoplasmic immunolabeling of MHC I. There are CD8-positive cells disseminated in the endomysium and rarely infiltrating non-necrotic muscle fibers. Muscle fiber infiltrated by a CD8-positive cell intensely overexpresses MHC I (CD8/MHC I complex).

immunofluorescence to MHC I (Figure 6B). No immunofluorescence was detected in sections incubated with PBS omitting the primary antibody.

Cytokine Expression

To molecularly characterize the inflammation in muscle samples, we evaluated inflammatory cytokine gene expression, including IFN-γ, LITAF, IL-6, IL-12A, and IL-17 (Figure 7). There were no differences in the expression of IFN-γ among macroscopic grades. The expression of LITAF was higher in grade 3 compared with grade 1 ($P< 0.01$) and grade 0 ($P< 0.01$). The expression of IL-6 was higher in grade 3 compared with grade 2 ($P< 0.0001$), grade 1 ($P< 0.0001$) and grade 0 ($P= 0.0001$). The expression of IL-17 was higher in grade 3 compared with grade 1 ($P< 0.05$) and grade 0 ($P< 0.05$).

The expression of LITAF was highly positively correlated with the WS grade ($r_s = 0.818$; $P< 0.001$), inflammation score ($r_s = 0.706$; $P< 0.01$) and mitochondrial alterations ($r_s = 0.702$; $P< 0.01$). LITAF expression was also moderately positively correlated with atrophy ($r_s =$

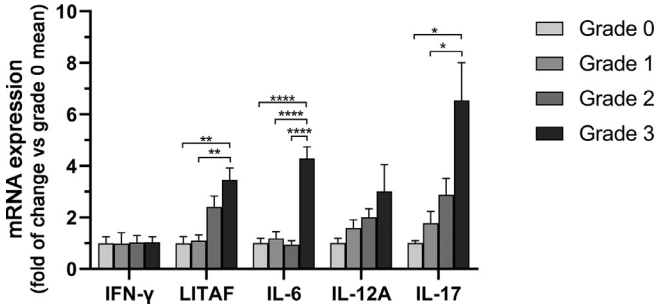

Figure 7. Quantitative RT-PCR analysis of inflammatory cytokine gene expression, in pectoralis muscle samples from 50 broiler chickens. Gene expression data are compared among samples with different macroscopic severity grades (grades 0-3, shown by different colored bars) based on 5 tested samples for each grade (20 samples total). Gene expression data are expressed as fold-change from normal muscle samples (grade 0). Bars indicate means ± SEM. There are no differences in the IFN-γ gene expression among the different macroscopic grades. LITAF, IL-6, IL-12α, and IL-17 gene expression was higher in grade 3 pectoralis muscle compared with less severe grades. The means were compared by one-way ANOVA and post-hoc Holm-Sidak's multiple comparison. Asterisks denote statistically differences between grades ($^*P < 0.05$, $^{**}P < 0.01$, $^{****}P < 0.0001$).

0.646; $P< 0.01$) and necrosis ($r_s = 0.586$; $P< 0.05$) and fibrosis ($r_s = 0.666$; $P< 0.01$). The expression of IL-6 was moderately positively correlated with the WS grade ($r_s= 0.559$; $P<0.05$), inflammation score ($r_s = 0.592$; $P< 0.01$), necrosis ($r_s = 0.624$; $P< 0.01$), mitochondrial alterations ($r_s = 0.505$; $P< 0.05$) and lowly positively correlated with fibrosis ($r_s = 0.486$; $P< 0.05$). The expression of IL-12A was moderately positively correlated with the atrophy ($r_s = 0.504$; $P< 0.05$), inflammation score ($r_s = 0.631$; $P< 0.01$), necrosis ($r_s = 0.529$; $P< 0.05$), fibrosis ($r_s = 0.569$; $P< 0.05$) and lowly positively correlated with mitochondrial alterations ($r_s = 0.497$; $P< 0.05$). The expression of IL-17 was highly positively correlated with the WS grade ($r_s= 0.808$; $P< 0.001$) and moderately positively correlated with inflammation score ($r_s = 0.633$; $P< 0.01$), necrosis ($r_s = 0.652$; $P< 0.01$), fibrosis ($r_s = 0.668$; $P< 0.01$), adipose tissue replacement ($r_s = 0.603$; $P< 0.05$) and mitochondrial alterations ($r_s = 0.607$; $P< 0.05$).

The correlations between gross lesions, histological, immunohistochemical and RT-PCR results were summarized in Supplementary Table 1.

DISCUSSION

WS is an emerging myopathy affecting broiler chicken pectoral and thigh muscles with an increasing incidence at slaughter-age in recent years (Kuttappan et al., 2017; Huang and Ahn, 2018; Malila et al., 2018). The morphologic appearance of this myopathy can adversely affect consumer acceptance of raw fillets and can cause a worsening of the chemical and textural properties of the meat, resulting in economic loss in the poultry industry (Kuttappan et al., 2016). Moreover, according to the OIE definition of animal welfare (OIE - World Organisation for Animal Health, 2019), there is a critical relationship between animal health and animal welfare, therefore this pathology can represent a serious welfare issue in live broilers (Kuttappan et al., 2016; Petracci et al., 2019).

The morphological and molecular characterization of this myopathy can lay the foundations for the development of genetic selection plans or therapies that may reduce the incidence of this condition with consequent reduction of the economic losses and improvement of animal welfare.

Our results showed that WS is a chronic necrotizing and inflammatory myopathy at slaughter-age, macroscopically characterized by white striations parallel to the muscle fibers (Kuttappan et al., 2016), and the striation thickness is related to the severity of the disease. WS was observed in 90% of the examined pectoralis muscles in our study, most commonly as a grade 1 lesion. The reported incidence of WS in broiler chicken varies between published works but the most recent reported incidence data of WS in Ross 308 vary from 75.5% to 97.8% at slaughter age (Huang and Ahn, 2018; Malila et al., 2018). Incidence data variation could depend on confounding factors such as strain, age, sex, feed etc. (Kuttappan et al., 2016).

Histological lesions were observed in all animals, both with and without macroscopic evidence of WS, suggesting that the underlying disease process is even more frequent than reported. Macroscopically unaffected chickens generally showed mild microscopic lesions and may represent early stages of the condition.

According to the authors' knowledge, this is the first study where inflammatory infiltrate associated with WS has been extensively characterized; until now, only the presence of CD3-positive T lymphocytes had been evaluated (Mazzoni et al., 2015). In the present study we showed that often the majority of the inflammatory cells were macrophages; we characterized the T cells subpopulations as mainly composed of CD8-positive cytotoxic T cells associated with less CD4-positive helper T cells and $\gamma\delta$-T cells; moreover, we reported the presence of a smaller number of Bu-1-positive B cells. Other already reported histologic findings (Kuttappan et al., 2013; Mazzoni et al., 2015), notably, myofiber atrophy, necrosis, fibrosis and replacement of skeletal muscles by adipose tissue, have been here associated with the WS degree.

The severity of the main histologic lesions was positively correlated with the macroscopic grade of WS. If we assume that higher grade of WS corresponds to more advanced states of the condition (Kuttappan et al., 2013), these data suggest concurrent progression of the histologic and macroscopic lesions in the pectoralis muscle. Inflammatory changes, fibrosis and adipose tissue replacement are the histologic lesions more strongly positively correlated with macroscopic grade of WS. This observation suggest that these lesions may be mainly responsible for the macroscopic aspect of WS in chicken muscles. These results are supported by other studies where the increased fat and decreased protein contents have been associated with the degree of white striping (Kuttappan et al., 2013).

The association between mitochondrial abnormalities and muscle inflammation is widely reported and it is frequently linked with damage of the mitochondrial DNA (Pagano et al., 2019). The grade of WS correlated with mitochondrial alterations suggesting a worsening of mitochondrial function according to the progression of the condition. In addition to an effect of inflammation, subsarcolemmal mitochondrial aggregates may also reflect chronic muscle hypoxia. It is reported that during hypoxia, skeletal muscle mitochondria shift position and localize preferentially in the subsarcolemmal region, where they are closer to capillaries. Moreover, the reduced COX-activity may reflect a hypoxia-related decrease in mitochondrial content, probably due to a combination of reduced mitochondrial biogenesis and increased mitophagy (Gamboa and Andrade, 2010). These findings are also supported by the reported increase in long- and medium-chain fatty acids and decrease in acylcarnitine esters in WS affected muscles, reflecting a defect in the beta-oxidation (Boerboom et al., 2018).

Although the macrophagic inflammatory infiltrate with abundant myofiber necrosis, fibrosis and mitochondrial abnormalities are consistent with a ischemia-induced myopathy (Gamboa and Andrade, 2010; Ghaly and Marsh, 2010), these morphological data alone are not sufficient to support the ischemic pathomechanism, however, they well fit into the existing literature (Boerboom et al., 2018; Marchesi et al., 2019; Malila et al., 2020).

We hypothesize that histiocytic inflammation is triggered mainly by necrosis due to muscle hypoxia (Boerboom et al., 2018). It has been suggested that the vascular system in broiler chicken muscles may be marginal, supporting muscle growth under steady state conditions, but inadequate to support the muscle under stress (Boerboom et al., 2018). In this scenario, small stresses, such as minor trauma or sudden movements of wings (Bianchi et al., 2006), might destabilize an already precarious equilibrium and incite the development of this necrotizing and histiocytic myositis. In addition to removing dead tissues and initiating the process of repair, macrophages can contribute to tissue injury in chronic inflammation by secreting cytokines and growth factors that act on various cells, notably T lymphocytes (Wigley and Kaiser, 2003; Fernández et al., 2017).

T_H1 cytokines, including IL-12 and IFN-γ, are involved in the induction of cell-mediated immunity (Wigley and Kaiser, 2003; Giansanti et al., 2007). In the present study, there were no differences in IFN-γ and IL-12 mRNA expression among different grades of WS suggesting a constant production of these cytokines during disease progression.

We showed that LITAF was overexpressed in high grade WS. LITAF is known as a TNF$-\alpha$ inducer in mammals (ZOU et al., 2015), however, in chickens the TNF$-\alpha$ homologous gene has been recently identified and the relationship with LITAF is not yet well defined (Hong et al., 2006; Rohde et al., 2018). Both in mammals and in chickens, LITAF stimulates the expression of TNF-like ligand 1A (Hong et al., 2006; Park et al., 2007; ZOU et al., 2015). TNF-like ligand 1A, also termed tumor necrosis factor superfamily member 15 and vascular endothelial growth inhibitor, is an important negative regulator for endothelial cell proliferation, which may result in inhibition of vasculogenesis (Zhang et al., 2017). This activity might be part of the pathogenesis of an ischemic muscle disease. This hypothesis is further supported by the positive correlation between LITAF expression and the observed necrosis and fibrosis. Moreover, the upregulation of LITAF expression is reported in different immune-mediated disorders in humans, such as inflammatory bowel disease and rheumatoid arthritis (ZOU et al., 2015).

We observed that IL-6 is overexpressed in high grade WS. IL-6 is generally considered a proinflammatory cytokine produced by T and B lymphocytes, macrophages and endothelial cells (Giansanti et al., 2007). However, at least in mammals, IL-6 can also be produced by skeletal muscle fibers after physical exercise and, in this case, exerts an anti-inflammatory action. Conversely, in an inflammatory microenvironment with other proinflammatory cytokines such as TNF-α, IL-6 promotes inflammation (Pedersen and Febbraio, 2008). Furthermore, the overproduction of IL-6 is considered important in the pathogenesis of multiple autoimmune inflammatory diseases, in which an imbalance between T_H17 cells and regulatory T cells and autoantibodies play a central role (Jones et al., 2018).

IL-17 is another proinflammatory cytokine overexpressed in high-grade WS and principally released by activated T lymphocytes, specifically CD4+ T_H17 and $\gamma\delta$-T cells. Moreover, IL-17 also induces IL-6 release by macrophages (Walliser and Göbel, 2018). The functions of IL-17 are not yet well characterized in birds but, as for IL-6 and LITAF, IL-17 in mammals has been linked to several immune-mediated diseases such as rheumatoid arthritis, multiple sclerosis, lupus and Crohn's disease (Tabarkiewicz et al., 2015; Walliser and Göbel, 2018). The IL-17 and IL-6 upregulation suggest an enhanced T_H17 response in severe degrees of WS (Tabarkiewicz et al., 2015). The enhancement of the T_H17 response has been widely reported during muscle (Gaines et al., 1999; Ege et al., 2004; Lopes et al., 2010) and myocardial ischemia (Saini et al., 2005) where it has a critical role in angiogenesis, repair and remodeling (Hata et al., 2011; Chen et al., 2018).

Whole transcriptome analysis of pectoralis major muscle of WS affected broilers already highlighted that the activation of immune system is one of the most relevant biological processes involved in this pathology, together with angiogenesis, hypoxia, cell death, striated muscle contraction and calcium signaling disturbances (Zambonelli et al., 2016; Marchesi et al., 2019; Malila et al., 2020). Specifically, consistent with our results, the overexpression of LITAF (Marchesi et al., 2019) in WS affected muscles and the absence of differential expression of IFN-γ and IL-12 have been reported (Marchesi et al., 2019; Malila et al., 2020). Differently, in the present study we also observed the overexpression of IL-6 and IL-17 in muscles with higher degree of WS, this difference may depend on several factors, including differences in the samples (genetic, age, feed, etc.) (Kuttappan et al., 2016), in study design, in the sensitivity and specificity of the technique used (Kogenaru et al., 2012), etc.

In addition to the overexpression of cytokines related to autoimmune inflammatory diseases, we also described morphologically non-necrotic MHC I-positive muscle fibers infiltrated by CD8-positive lymphocytes (CD8/MHC I complex), the hallmark of immune-mediated inflammatory myopathy in human, dogs, sheep, and horses (Paciello et al., 2007, 2009; Pasolini et al., 2018; Pagano et al., 2019). An association between ischemic injuries and immune-mediated disorders has been described in humans during myocardial infarctions (Liao and Cheng, 2006), stroke, and traumatic brain injury (Javidi and Magnus, 2019). Thus, an immune-mediated mechanism should be considered as a

component of the pathogenesis of the WS. We hypothesize that muscle necrosis might cause the release or the exposure of normally sequestered antigenic constituents that could potentially trigger an adaptive autoimmune response. Moreover, the persistent proinflammatory microenvironment following ischemic injuries could favor autoimmune responses to muscle antigens breaking tolerance mechanisms and triggering an immune-mediated myopathy (Liao and Cheng, 2006; Javidi and Magnus, 2019).

Our data are compatible with hypoxia-related damage to muscle tissue in WS, but further studies should consider other potential contributing mechanisms. In the present study, an immune-mediated component of the pathogenetic mechanism of WS has been suggested. Further studies are needed to evaluate the presence of circulating autoantibodies against muscle-antigens or the presence of autoreactive T cells (Tabarkiewicz et al., 2015; Javidi and Magnus, 2019).

CONCLUSIONS

WS is a frequent chronic necrotizing and inflammatory myopathy of broiler chickens at slaughter-age. Macroscopically, it is characterized by white striation parallel to the muscle fibers. Histological lesions were observed in all broiler chickens examined in this study, both with and without macroscopic evidence of WS. Histologically, WS muscles showed a multifocal to coalescing endomysial and perivascular inflammatory infiltrates mainly composed of macrophages and CD8-positive T lymphocytes with severe myofiber atrophy, necrosis, fibrosis and replacement by adipose tissue. Other associated myopathic changes were endomysial and perimysial edema, centralization of nuclei, and fiber splitting, and there were a diffuse sarcoplasmic and sarcolemmal overexpression of MHC I. The severity of the histologic lesions was positively correlated with the macroscopic degree of white striations. The data suggest that the striations were mainly composed of inflammatory cells, fibrous and adipose tissue. The observation of CD8/MHC I complexes, together with the higher expression of IL-6, IL-17, and LITAF in severe WS, suggest an immune-mediated component may contribute to this myopathy. Given the increase in incidence of WS, there is a pressing need to find a solution to reduce the incidence of WS and other hypoxia-related myopathies of broiler chickens both to reduce economic losses in the poultry industry and for the chicken's welfare. Moreover, further studies are needed to explore the immune-mediated component of WS pathogenesis.

ACKNOWLEDGMENTS

We thank Raffaele Ilsami for the excellent technical assistance. The author(s) received no financial support for the research, authorship, and/or publication of this article.

AUTHOR CONTRIBUTIONS

F. P. and O. P. conceived and designed the study; F. P., D. D. B., G. P., I. d'A., A. L., and F. C. performed the experiments; F. P. and O. P. analyzed and interpreted the data; F. P. drafted the manuscript; O. P., R. M., L. D. and S. P. critically revised the manuscript; S. P. and O. P. provided resources and supervised the study. All authors have read and approved the manuscript.

DISCLOSURES

The author(s) declared no potential conflicts of interest with respect to the research, authorship, and/or publication of this article.

SUPPLEMENTARY MATERIALS

Supplementary material associated with this article can be found, in the online version, at doi:10.1016/j.psj.2021.101150.

REFERENCES

Aickin, M., and H. Gensler. 1996. Adjusting for multiple testing when reporting research results: the Bonferroni vs Holm methods. Am. J. Public Health 86:726–728.

Bailey, R. A., K. A. Watson, S. F. Bilgili, and S. Avendano. 2015. The genetic basis of pectoralis major myopathies in modern broiler chicken lines. Poult. Sci. 94:2870–2879.

Bianchi, M., M. Petracci, A. Franchini, and C. Cavani. 2006. The occurrence of deep pectoral myopathy in roaster chickens. Poult. Sci. 85:1843–1846.

De Biase, D., G. Piegari, F. Prisco, I. Cimmino, C. Pirozzi, G. Mattace Raso, F. Oriente, E. Grieco, S. Papparella, and O. Paciello. 2020. Autophagy and NLRP3 inflammasome crosstalk in neuroinflammation in aged bovine brains. J. Cell. Physiol. 235:5394–5403.

Boerboom, G., T. van Kempen, A. Navarro-Villa, and A. Pérez-Bonilla. 2018. Unraveling the cause of white striping in broilers using metabolomics. Poult. Sci. 97:3977–3986.

Chen, Z., W. Yan, Y. Mao, Y. Ni, L. Zhou, H. Song, W. Xu, L. Wang, and Y. Shen. 2018. Effect of aerobic exercise on treg and Th17 of rats with ischemic cardiomyopathy. J. Cardiovasc. Transl. Res. 11:230–235.

Cimmino, I., F. Margheri, F. Prisco, G. Perruolo, V. D'Esposito, A. Laurenzana, G. Fibbi, O. Paciello, N. Doti, M. Ruvo, C. Miele, F. Beguinot, P. Formisano, and F. Oriente. 2019. Prep1 regulates angiogenesis through a PGC-1α–mediated mechanism. FASEB J. fj.201901230RR.

Costagliola, A., S. Wojcik, T. B. Pagano, D. De Biase, V. Russo, V. Iovane, E. Grieco, S. Papparella, and O. Paciello. 2016. Age-related changes in skeletal muscle of cattle. Vet. Pathol. 53:436–446.

Dubowitz, V., C. A. Sewry, A. Oldfors, and R. J. M. Lane. 2013. Muscle Biopsy: A Practical Approach 4th ed. Saunders.

Ege, T., M. H. Us, M. Sungun, and E. Duran. 2004. Cytokine response in lower extremity ischaemia/reperfusion. J. Int. Med. Res. 32:124–131.

Fernández, M., J. Benavides, P. Castaño, N. Elguezabal, M. Fuertes, M. Muñoz, M. Royo, M. C. Ferreras, and V. Pérez. 2017. Macrophage subsets within granulomatous intestinal lesions in bovine paratuberculosis. Vet. Pathol. 54:82–93.

Gaines, G. C., M. B. Welborn, L. L. Moldawer, T. S. Huber, T. R. S. Harward, and J. M. Seeger. 1999. Attenuation of skeletal muscle ischemia/reperfusion injury by inhibition of tumor necrosis factor. J. Vasc. Surg. 29:370–376.

Gamboa, J. L., and F. H. Andrade. 2010. Mitochondrial content and distribution changes specific to mouse diaphragm after chronic

normobaric hypoxia. Am. J. Physiol. - Regul. Integr. Comp. Physiol. 298:575–583.
Ghaly, A., and D. R. Marsh. 2010. Ischaemia-reperfusion modulates inflammation and fibrosis of skeletal muscle after contusion injury. Int. J. Exp. Pathol. 91:244–255.
Giansanti, F., M. Giardi, and D. Botti. 2007. Avian cytokines - an overview. Curr. Pharm. Des. 12:3083–3099.
Hata, T., M. Takahashi, S. Hida, M. Kawaguchi, Y. Kashima, F. Usui, H. Morimoto, A. Nishiyama, A. Izawa, J. Koyama, Y. Iwakura, S. Taki, and U. Ikeda. 2011. Critical role of Th17 cells in inflammation and neovascularization after ischaemia. Cardiovasc. Res. 90:364–372.
Hong, Y. H., H. S. Lillehoj, S. Hyen Lee, D. Woon Park, and E. P. Lillehoj. 2006. Molecular cloning and characterization of chicken lipopolysaccharide-induced TNF-α factor (LITAF). Dev. Comp. Immunol. 30:919–929.
Huang, X., and D. U. Ahn. 2018. The Incidence of muscle abnormalities in broiler breast meat − a review. Korean J. Food Sci. Anim. Resour. 38:835–850.
Javidi, E., and T. Magnus. 2019. Autoimmunity after ischemic stroke and brain injury. Front. Immunol. 10:1–12.
Johnson, S. J., and F. R. Walker. 2015. Strategies to improve quantitative assessment of immunohistochemical and immunofluorescent labelling. Sci. Rep. 5:3–6.
Jones, B. E., M. D. Maerz, and J. H. Buckner. 2018. IL-6: a cytokine at the crossroads of autoimmunity. Curr. Opin. Immunol. 55:9–14.
Kogenaru, S., Y. Qing, Y. Guo, and N. Wang. 2012. RNA-seq and microarray complement each other in transcriptome profiling. BMC Genom. 13:629.
Kuttappan, V. A., B. M. Hargis, and C. M. Owens. 2016. White striping and woody breast myopathies in the modern poultry industry: a review. Poult. Sci. 95:2724–2733.
Kuttappan, V. A., C. M. Owens, C. Coon, B. M. Hargis, and M. Vazquez-Añon. 2017. Incidence of broiler breast myopathies at 2 different ages and its impact on selected raw meat quality parameters. Poult. Sci. 96:3005–3009.
Kuttappan, V. A., H. L. Shivaprasad, D. P. Shaw, B. A. Valentine, B. M. Hargis, F. D. Clark, S. R. McKee, C. M. Owens, V. A. Kuttappan, B. M. Hargis, F. D. Clark, C. M. Owens, D. P. Shaw, and H. L. Shivaprasad. 2013. Pathological changes associated with white striping in broiler breast muscles. Poult. Sci. 92:331–338.
Lama, A., C. Annunziata, L. Coretti, C. Pirozzi, F. Di Guida, A. Nitrato Izzo, C. Cristiano, M. P. Mollica, L. Chiariotti, A. Pelagalli, F. Lembo, R. Meli, and G. Mattace Raso. 2019. N-(1-carbamoyl-2-phenylethyl) butyramide reduces antibiotic-induced intestinal injury, innate immune activation and modulates microbiota composition. Sci. Rep. 9:4832.
Law, A. M. K., J. X. M. Yin, L. Castillo, A. I. J. Young, C. Piggin, S. Rogers, C. E. Caldon, A. Burgess, E. K. A. Millar, S. A. O'Toole, D. Gallego-Ortega, C. J. Ormandy, and S. R. Oakes. 2017. Andy's algorithms: new automated digital image analysis pipelines for FIJI. Sci. Rep. 7:1–11.
Liao, Y. H., and X. Cheng. 2006. Autoimmunity in myocardial infarction. Int. J. Cardiol. 112:21–26.
Lopes, R. D., M. L. Batista, J. C. Rosa, F. S. De Lira, E. Martins, A. Y. Shimura, P. C. Brum, A. H. Lancha, M. C. L. Seelaender, and A. C. Lopes. 2010. Changes in the production of IL-10 and TNF-α in skeletal muscle of rats with heart failure secondary to acute myocardial infarction (Arquivos Brasileiros de Cardiologia (2010) 94, 3, (313-320)). Arq. Bras. Cardiol. 95:279.
Malila, Y., K. Thanatsang, S. Arayamethakorn, T. Uengwetwanit, Y. Srimarut, M. Petracci, G. M. Strasburg, W. Rungrassamee, and W. Visessanguan. 2019. Absolute expressions of hypoxia-inducible factor-1 alpha (HIF1A) transcript and the associated genes in chicken skeletal muscle with white striping and wooden breast myopathies. PLoS One 14:1–23.
Malila, Y., J. U-Chupaj, Y. Srimarut, P. Chaiwiwattrakul, T. Uengwetwanit, S. Arayamethakorn, V. Punyapornwithaya, C. Sansamur, C. P. Kirschke, L. Huang, S. Tepaamorndech, M. Petracci, W. Rungrassamee, and W. Visessanguan. 2018. Monitoring of white striping and wooden breast cases and impacts on quality of breast meat collected from commercial broilers (Gallus gallus). Asian-Australasian J. Anim. Sci. 31:1807–1817.
Malila, Y., T. Uengwetwanit, S. Arayamethakorn, Y. Srimarut, K. V. Thanatsang, F. Soglia, G. M. Strasburg, W. Rungrassamee, and W. Visessanguan. 2020. Transcriptional profiles of skeletal muscle associated with increasing severity of white striping in commercial broilers. Front. Physiol. 11:1–16.
Marchesi, J. A. P., A. M. G. Ibelli, J. O. Peixoto, M. E. Cantão, J. R. C. Pandolfi, C. M. M. Marciano, R. Zanella, M. L. Settles, L. L. Coutinho, and M. C. Ledur. 2019. Whole transcriptome analysis of the pectoralis major muscle reveals molecular mechanisms involved with white striping in broiler chickens. Poult. Sci. 98:590–601.
Mazzoni, M., M. Petracci, A. Meluzzi, C. Cavani, P. Clavenzani, and F. Sirri. 2015. Relationship between pectoralis major muscle histology and quality traits of chicken meat. Poult. Sci. 94:123–130.
Meuten, D. J., F. M. Moore, and J. W. George. 2016. Mitotic count and the field of view area. Vet. Pathol. 53:7–9.
Meyerholz, D. K., N. L. Tintle, and A. P. Beck. 2019. Common pitfalls in analysis of tissue scores. Vet. Pathol. 56:39–42.
Mukaka, M. M. 2012. Statistics corner: A guide to appropriate use of correlation coefficient in medical research. Malawi Med. J. 24:69–71.
OIE - World Organisation for Animal Health. 2019. Chapter 7.1. Introduction to the recommendations for animal welfare. Terrestrial Animal Health Code. Accessed Feb. 2021. https://www.oie.int/index.php?id=169&L = 0&htmfile=chapitre_aw_introduction.htm.
Paciello, O., G. Oliva, L. Gradoni, L. Manna, V. F. Manzillo, S. Wojcik, F. Trapani, and S. Papparella. 2009. Canine inflammatory myopathy associated with leishmania infantum infection. Neuromuscul. Disord. 19:124–130.
Paciello, O., and S. Papparella. 2009. Histochemical and immunohistological approach to comparative neuromuscular diseases. Folia Histochem. Cytobiol. 47:143–152.
Paciello, O., G. D. Shelton, and S. Papparella. 2007. Expression of major histocompatibility complex class I and class II antigens in canine masticatory muscle myositis. Neuromuscul. Disord. 17:313–320.
Pagano, T. B., F. Prisco, D. De Biase, G. Piegari, M. P. Maurelli, L. Rinaldi, G. Cringoli, S. Papparella, and O. Paciello. 2020. Muscular sarcocystosis in sheep associated with lymphoplasmacytic myositis and expression of major histocompatibility complex class I and II. Vet. Pathol. 57:272–280.
Pagano, T. B., S. Wojcik, A. Costagliola, D. De Biase, S. Iovino, V. Iovane, V. Russo, S. Papparella, and O. Paciello. 2015. Age related skeletal muscle atrophy and upregulation of autophagy in dogs. Vet. J. 206:54–60.
Park, S. S., H. S. Lillehoj, Y. H. Hong, and S. H. Lee. 2007. Functional characterization of tumor necrosis factor superfamily 15 (TNFSF15) induced by lipopolysaccharides and Eimeria infection. Dev. Comp. Immunol. 31:934–944.
Pasolini, M. P., T. B. Pagano, A. Costagliola, D. De Biase, B. Lamagna, L. Auletta, G. Fatone, M. Greco, P. Coluccia, V. Veneziano, C. Pirozzi, G. M. Raso, P. Santoro, G. Manna, S. Papparella, and O. Paciello. 2018. Inflammatory myopathy in horses with chronic piroplasmosis. Vet. Pathol. 55:133–143.
Pedersen, B. K., and M. A. Febbraio. 2008. Muscle as an endocrine organ: focus on muscle-derived interleukin-6. Physiol. Rev. 88:1379–1406.
Petracci, M., F. Soglia, M. Madruga, L. Carvalho, E. Ida, and M. Estévez. 2019. Wooden-breast, white striping, and spaghetti meat: causes, consequences and consumer perception of emerging broiler meat abnormalities. Compr. Rev. Food Sci. Food Saf. 18:565–583.
Praud, C., J. Jimenez, E. Pampouille, N. Couroussé, E. Godet, E. Le Bihan-Duval, and C. Berri. 2020. Molecular phenotyping of white striping and wooden breast myopathies in chicken. Front. Physiol. 11:1–16.
Prisco, F., S. Papparella, and O. Paciello. 2020. The correlation between cardiac and skeletal muscle pathology in animal models of idiopathic inflammatory myopathies. Acta Myol. XXXIX:315–321.
Rohde, F., B. Schusser, T. Hron, H. Farkašová, J. Plachý, S. Härtle, J. Hejnar, D. Elleder, and B. Kaspers. 2018. Characterization of chicken tumor necrosis factor-α, a long missed cytokine in birds. Front. Immunol. 9:1–14.

Saini, H. K., Y. J. Xu, M. Zhang, P. P. Liu, L. A. Kirshenbaum, and N. S. Dhalla. 2005. Role of tumour necrosis factor-alpha and other cytokines in ischemia-reperfusion-induced injury in the heart. Exp. Clin. Cardiol. 10:213–222.

Salles, G. B. C., M. M. Boiago, A. D. Silva, V. M. Morsch, A. Gris, R. E. Mendes, M. D. Baldissera, and A. S. da Silva. 2019. Lipid peroxidation and protein oxidation in broiler breast fillets with white striping myopathy. J. Food Biochem. 43:1–7.

Smith, D. P., and D. L. Fletcher. 1988. Chicken breast muscle fiber type and diameter as influenced by age and intramuscular location. Poult. Sci. 67:908–913.

Tabarkiewicz, J., K. Pogoda, A. Karczmarczyk, P. Pozarowski, and K. Giannopoulos. 2015. The Role of IL-17 and Th17 lymphocytes in autoimmune diseases. Arch. Immunol. Ther. Exp. (Warsz). 63:435–449.

Walliser, I., and T. W. Göbel. 2018. Chicken IL-17A is expressed in $\alpha\beta$ and $\gamma\delta$ T cell subsets and binds to a receptor present on macrophages, and T cells. Dev. Comp. Immunol. 81:44–53.

Wigley, P., and P. Kaiser. 2003. Avian cytokines in health and disease. Rev. Bras. Ciência Avícola 5:1–14.

Zaghini, A., G. Sarli, C. Barboni, M. Sanapo, V. Pellegrino, A. Diana, N. Linta, J. Rambaldi, M. R. D'Apice, M. Murdocca, M. Baleani, F. Baruffaldi, R. Fognani, R. Mecca, A. Festa, S. Papparella, O. Paciello, F. Prisco, C. Capanni, M. Loi, E. Schena, G. Lattanzi, and S. Squarzoni. 2020. Long term breeding of the Lmna G609G progeric mouse: characterization of homozygous and heterozygous models. Exp. Gerontol. 130:110784.

Zambonelli, P., M. Zappaterra, F. Soglia, M. Petracci, F. Sirri, C. Cavani, and R. Davoli. 2016. Detection of differentially expressed genes in broiler pectoralis major muscle affected by White Striping − Wooden Breast myopathies. Poult. Sci. 95:2771–2785.

Zanetti, M. A., D. C. Tedesco, T. Schneider, S. T. F. Teixeira, L. Daroit, F. Pilotto, E. L. Dickel, S. P. Santos, and L. R. Dos Santos. 2018. Economic losses associated with Wooden Breast and White Striping in broilers. Semin. Agrar. 39:887–891.

Zhang, Z. H., Q. Z. Chen, F. Jiang, T. A. Townsend, C. J. Mao, C. Y. You, W. H. Yang, Z. Y. Sun, J. G. Yu, and H. Yan. 2017. Changes in TL1A levels and associated cytokines during pathogenesis of diabetic retinopathy. Mol. Med. Rep. 15:573–580.

Zou, J., P. Guo, N. Lv, and D. Huang. 2015. Lipopolysaccharide-induced tumor necrosis factor-α factor enhances inflammation and is associated with cancer (Review). Mol. Med. Rep. 12:6399–6404.